Gauss-Newton Method for Segmentation assisted Deformable Registration

Miro Jurisic[1], Tobias Fechter[2], Frida Hauler[1], Hugo Furtado[1,3], Ursula Nestle[2], and Wolfgang Birkfellner[1,3]

[1] Medical University of Vienna, Center for Medical Physics and Biomedical Engineering, Vienna Austria
miro.jurisic@meduniwien.ac.at
[2] University Hospital Freiburg, Department of Radiation Oncology, Freiburg im Breisgau, Germany.
[3] Medical University of Vienna, Christian Doppler Laboratory for Medical Radiation Research for Radiation Oncology, Vienna Austria

Abstract. In this work, we try to develop a fast converging method for segmentation assisted deformable registration. The segmentation step consists of a piece-wise constant Mumford-Shah energy model while registration is driven by the sum of squared distances of both initial images and segmented mask with a diffusion regularization. In order to solve this energy minimization problem, a second order Gauss-Newton optimization method is used. For the numerical experiments we used CT data sets from the EMPIRE10 challenge. In this preliminary study, we show high accuracy of our algorithm.

Keywords: energy based segmentation, deformable registration, Gauss-Newton method

1 Introduction

Deformable image registration is an important image processing method in radiotherapy. In case of image guided radiotherapy, registration helps to improve precision and accuracy of the delivery of the radiation. It tries to correct for the movement of the patient and for the natural deformation of the human anatomy, for example lung deformation during breathing or weight loss. Since the real anatomical movements come from complex internal forces within and between organs as well as forces applied to the body from outside, we try to simulate forces by simplified models. In order to build these models, registration algorithms estimate the forces from the deformations observed in the images. We can separate deformable registration methods to those that estimate forces at each image point at each voxel and those that estimate forces on some specific locations from which they interpolate forces to the remainder of the image [1] [2]. Both of these methods in their original papers are based only on the intensities of images. A large number of methods are developed based on these two methods that try to increase accuracy by the extraction of features from the images

such as edges, gradients [3], high dimensional descriptors [4] or even high-level methods for segmentation of the specific anatomical locations [5]. Most of these methods require preprocessing step to extract targeting features.
Our work present solution for the simultaneous segmentation and registration in order to avoid spending time for feature extraction. The important contribution of our work is the introduction of the second order Gauss-Newton optimization method for minimization of the joint segmentation and registration energy in comparison to the variational method [6].

2 Gauss-Newton optimization

Gauss-Newton method belongs to the second order optimization methods because it approximates the second order derivative of the energy. It deals with the least squares problem of the form

$$f(\boldsymbol{x}) = \frac{1}{2}\sum_{i=1}^{m} r_i^2(\boldsymbol{x}), \tag{1}$$

where r_i is a smooth function from R^n to R and we assume that $m > n$. The goal of the method is to find minima of the function f. We proceed first by building a vector $\boldsymbol{r}$ from individual functions r_j

$$\boldsymbol{r} = (r_1, r_2, ..., r_m)^T. \tag{2}$$

Now we can rewrite function f in a form $f(x) = \frac{1}{2}|r(x)|_2^2$. The derivatives of function $f(x)$ can be expressed with Jacobian $J(x)$

$$J_{j,i}(x) = \frac{\partial r_j}{\partial x_i}. \tag{3}$$

The standard Newton optimization method tends to solve (1) using an iterative method

$$x_{k+1} = x_k + \alpha_k p_k;\ \nabla^2 f(x) p_k = -\nabla f(k) \tag{4}$$

where the positive scalar α_k is called the step length. Since 4 include the calculation of second derivatives of functions r_j which can be computationally expensive, we use a Gauss-Newton approximation for the Hessian of function

$$\nabla^2 f(x) \approx J(x)^T J(x). \tag{5}$$

which leads to

$$J(x)^T J(x) p_k = -J(x)^T r(x). \tag{6}$$

2.1 Segmentation

Segmentation is one of the most fundamental image processing methods. It tries to separate regions of interest in the images. Our approach include energy minimization segmentation based on Mumford-Shah energy [7] of the form

$$E(c_{in}, c_{out}, H) = \sum_{\Omega}(c_{in} - u_0)^2 H + \sum_{\Omega}(c_{out} - u_0)^2(1 - H) \tag{7}$$

where c_{in} is average value inside contoured object, c_{out} is average value outside the contoured object,$\sum_{\Omega}$ is image space and H is a Heaviside function that has value 1 inside object and 0 outside object.

Gauss-Newton Segmentation In order to use Gauss-Newton approach which deals with least-squared type of problems, we introduced the energy function SG

$$SG = \frac{1}{2}\sum_{\Omega}\left(\lambda[m(c,\phi) - M]^2 dx + \alpha|\nabla\phi|^2 + \lambda K(\phi)^2\right) \tag{8}$$

where $m(c,\phi)$ is the modelling image M is the modelled image. ϕ is defined by

$$\phi = i \text{ in } \Omega_i \tag{9}$$

and represent the masking image, where each region Ω_i represents a different integer value i. The modelling image is defined by the masking image and by an average value inside the region:

$$m(c,\phi) = \sum_{i=1}^{n} c_i\psi_i; \quad \psi_i = \frac{1}{\alpha_i}\prod_{j=1,j\neq i}^{n}(\phi - j) \tag{10}$$

Next to the regularization term $\alpha|\nabla\phi|^2$ we introduce another regularization term $K(\phi)$. This term has the task of penalizing non-integer values of ϕ:

$$K(\phi) = \prod_{i}(\phi - i) \tag{11}$$

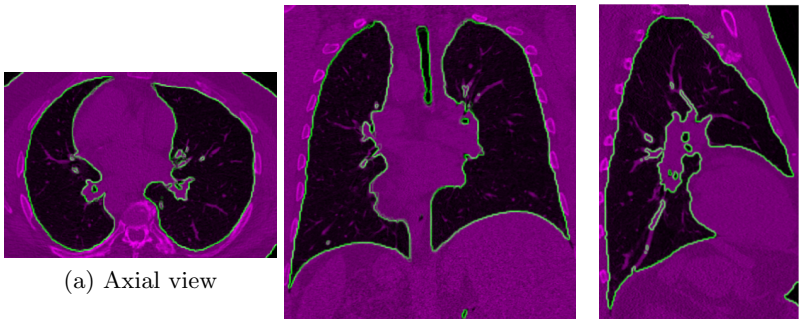

(a) Axial view (b) Sagital view (c) Coronal view

Fig. 1: This figure shows an overlap of the segmentation mask (green line) generated during the segmentation assisted registration

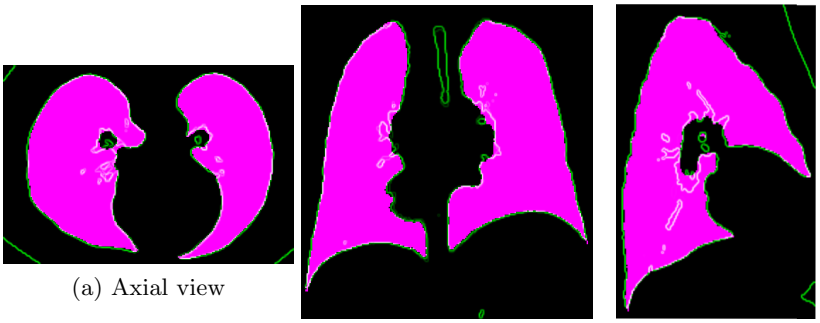

(a) Axial view (b) Sagital view (c) Coronal view

Fig. 2: This figure shows an overlap of the segmentation mask (green line) generated during the segmentation assisted registration with ground truth masks (purple) from EMPIRE10 data set

2.2 Registration

As already mentioned, deformable registration can be seen as an optimization method of an appropriate energy function. The mathematical formulation of the registration problem [8] is

$$E_{reg}(\boldsymbol{x}, \boldsymbol{u}) = S(\boldsymbol{x}, \boldsymbol{u}) + \alpha R(\boldsymbol{u}) \tag{12}$$

where S is the similarity measure and R is the regularization term. If we take the assumption that the similar objects in two images have the same intensity value, we can use the sum of squared distances as a similarity measure. Our similarity measure is therefore given by

$$S(\boldsymbol{x}, \boldsymbol{u}) = \frac{1}{2} \sum_{\Omega} (I_1(\boldsymbol{x} - I_2(\boldsymbol{x} + \boldsymbol{u}))^2 \tag{13}$$

For regularization term we use sum of squares of deformation field component gradient, known as diffusion regularization [9]

$$R(\boldsymbol{u}) = \frac{1}{2} \sum_{\Omega} \sum_{i=1}^{3} |\boldsymbol{\nabla} u_i|^2 \tag{14}$$

where u_i is ith component of the deformation field.

3 Segmentation assisted Registration

The main problem consist of setting the correct energy function. If we start with a problem where we do not have any prior information about the images and no prior segmentation masks, we need to choose the energy function that simultaneously segments both images. In this case, the joint segmentation and registration

energy function E_{joint} consists of the diffusion registration E_{reg},the segmentation of fixed image $SG(F)$,the segmentation of moving image $SG(M)$ and an extra similarity term in form of sum of squared distances between segmented masks $\phi_m^*(\boldsymbol{u})$ and ϕ_f

$$E_{joint} = E_{reg} + SG(F) + SG(M) + \frac{1}{2}\sum_{\Omega}\left(\phi_m^*(\boldsymbol{u}) - \phi_f\right)^2. \tag{15}$$

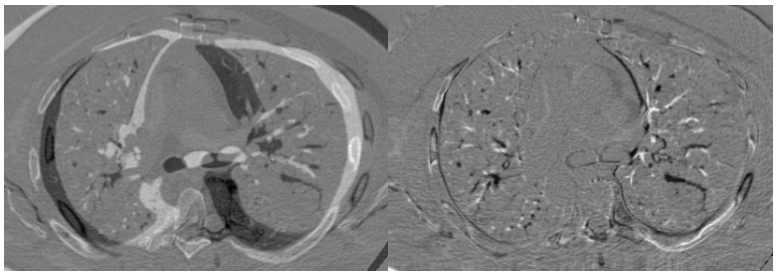

(a) before registration (b) after registration

Fig. 3: An example of inhale and exhale subtracted volumes in axial view before and after registration

4 Experiments

For the numerical experiments we used publicly available EMPIRE10 data set [10]. This data set contains 30 inhale and exhale pairs of the pulmonary computed tomography scans (CT). This data set contains also ground truth segmentation mask for the each CT volume. These masks are used to asses registration accuracy. We have randomly selected 10 pairs for our experiments with the initial dice score ranging from 0.598 until 0.940. In table 1 we show the dice scores for selected data pair ordered by the dice score before deformable registration. From this table we can notice that after the registration in each case the dice score is above 89%. Surprisingly the highest dice score after registration does not come for data pair 17, which has high initial overlap, it is data pair 22 with the highest dice score of 98.3%.
Concerning the parameters and the initial configuration of the iterative method, we used a zeros initial deformation field, an all ones initial segmentation masks for both ϕ_m and ϕ_f, and we used for the constants values $\alpha = 0.05$, $\lambda = 0.1$ and $n = 2$ selected to achieve the highest dice scores.

Table 1: Dice score accuracy of DIR

Pair	21	16	28	30	7	10	11	22	23	17
Before	0.598	0.702	0.733	0.756	0.776	0.829	0.847	0.877	0.890	0.940
After	0.896	0.962	0.956	0.976	0.958	0.935	0.963	0.983	0.970	0.980

(a) before registration (b) after registration

Fig. 4: An example of inhale and exhale subtracted volumes in sagital view before and after registration

5 Notes and Comments

We have presented preliminary work on implementation of Gauss-Newton optimization method for segmentation assisted registration. This method has a high accuracy for the pulmonary data registration using a dice score as an accuracy measure. Segmentations created during the deformable registration have high overlap (only visual inspection) with the ground truth segmentation masks from the data set. The main difference from the standard segmentation methods is that the segmentation in our case is not targeted at the specific organ. It targets a homogeneous areas. In the case of the lung CT, our segmentation tends to separate the tissue from the air. If we take a look at the Figures 1 and 2, we can notice that our segmentation selects also some big vessels inside the lung. Even though, it would be interesting to connect this approach to the recent work for sliding organ motion [11], where authors use lung masks to predict location of discontinuities in the deformation field. It would be also interesting for the future work to apply this segmentation method to the anatomical site without

large air volumes, like pelvic area and to check can the algorithm distinguish between the different tissues. Unfortunately our work did not include comparison to the other methods, but by using publicly available data and by publishing results with the pair numbers (see table 1), we try to overcome this shortcoming of the presented research. While our validation was focused on CT of the pulmonary data, we believe that our approach can be used also for CT to CBCT registration which is an important task in the radiotherapy environment. We also believe that the coupling segmentation and registration can gain not only in the accuracy, but also in the robustness of the registration, specially in the case of larger deformations like at data pair 21. Our future work will include validation of our deformable registration method with landmark distance error, application to other anatomical sites, as well as application to registration of the other imaging modalities.

6 Acknowledgement

This research received funding from the European Union Seventh Framework Programme (FP7-PEOPLE-2011-ITN) under grant agreement PITN-GA-2011-290148. It is a part of ITN project called Software for the Use of Multi-Modality images in External Radiotherapy (SUMMER).

References

1. J.-P. Thirion: Image matching as a diffusion process: an analogy with Maxwells demons. Medical Image Analysis (1998) volume 2, number 3, pp 243260
2. D. Rueckert, L. I. Sonoda, and C. Hayes: Nonrigid registration using free-form deformations: Application to breast MR images. IEEE Transactions on Medical Imaging, 18/8 712, 1999.
3. Pluim, J., Maintz, J.B., Viergever, M.: Image registration by maximization of combined mutual information and gradient information. MICCAI 2000 , 103129.
4. M. P. Heinricha, M. Jenkinson, M. Bhushana, , T. Matind, F. V. Gleesond, Sir M. Bradyc, J. A. Schnabela: MIND: Modality independent neighbourhood descriptor for multi-modal deformable registration. Medical Image Analysis Volume 16, Issue 7, October 2012, Pages 14231435
5. L.H. Staib, and J.S. Duncan: Boundary Finding with Parametrically Deformable Models. PAMI, vol. 14, no. 11, pp. 10611075, 1992.
6. A. Yezzi, L. Zollei, T. Kapur: A variational framework for integrating segmentation and registration through active contours. Medical Image Analysis 7 (2003) 171185
7. D. Mumford and J. Shah.: Optimal approximation by piecewise smooth functions and associated variational problems. Commun. Pure Appl. Math., 42:577685, 1989.
8. A. Sotiras ,C. Davatzikos ,N. Paragios: Deformable Medical Image Registration: A Survey. Medical Imaging, IEEE Transactions on,2013 (1153-1190)
9. J. Modersitzki: Numerical Methods for Image Registration. Oxford University Press, New York, 2004.
10. Murphy et al. : Evaluation of registration methods on thoracic CT: the EMPIRE10 challenge. IEEE Trans Med Imaging. 2011 Nov;30(11):1901-20.

11. D.F. Pace, S.R. Aylward, M. Niethammer : A locally adaptive regularization based on anisotropic diffusion for deformable image registration of sliding organs. IEEE Trans Med Imaging. 2013 Nov;32(11):2114-26.